JASMAC Conference of the Japan Society of Microgravity Application

OR3-4

離散要素法を用いた粉粒体間付着力の重力依存性解析

Gravitational Dependency Analysis on Adhesive Force of Granular Material using a Discrete Element Method

大村拓也，濵﨑塁，石上玄也，
Takuya OMURA, Rui HAMASAKI, and Genya ISHIGAMI
慶應義塾大学，Keio University

1. Introduction

Solar rocky bodies, including Mars, the Moon, and asteroids, are covered with a fine granular material called regolith. This powdery surface layer significantly impacts the risks and challenges of space missions that utilize exploratory rovers and spacecraft. For example, NASA's Spirit Rover could not continue further exploration because its wheels were trapped in Martian regolith[1]. During the Apollo 12 lunar landing, scattered regolith exhaust from the landing engine damaged the Lunar Surveyor 3[2]. The maximum velocity of the scattered regolith was estimated as being as much as 2000 m/s[3]. Therefore, understanding the characteristics of regolith, particularly its gravitational dependency, is not only an area of scientific curiosity but also has practical significance. Clarifying these characteristics provides direct input into the design of rovers and spacecrafts and enhances their reliability and effectiveness, which are essential attributes for successful space missions.

Previous studies have utilized parabolic flights to analyze the static characteristics of the granular material[4,5]. These showed that the angle of repose was constant, regardless of gravity. However, inherent challenges of parabolic flights, such as their short duration and instability in experiments, are significant drawbacks. Ozaki et al.[6] conducted experiments at the International Space Station (ISS) to examine the characteristics of granular materials under stable artificial gravity conditions for long periods. Although these studies have yielded innovative insights, they have yet to be fully utilized in the numerical analysis of rovers or spacecrafts. This is because they still need to clarify the gravitational dependency of the characteristic parameters to represent granular materials, which is required for numerical analysis.

In response, our study utilized the ISS experimental results as the foundation for conducting simulations using the discrete element method (DEM). We analyzed the gravitational dependency characteristics of alumina beads by focusing on adhesive forces such as van der Waals and electrostatic forces between particles. First, we determined the basic DEM parameters based on the soil test results conducted on Earth. Next, by adjusting the adhesion parameters in our simulation to align with the ISS experimental results, we identified the gravitational dependency of the adhesive force between the alumina beads. The purpose of this study is to clarify the gravitational dependency of the DEM parameters to represent granular materials in numerical simulations, in order to use them in numerical analysis of rovers or spacecrafts. The rest of this paper is organized as follows: Section 2 describes the calibration method and results for the DEM parameters based on the soil test results. Section 3 presents an overview of the ISS experiments and compares the experimental and simulation results, focusing on the behavior of alumina beads under various artificial gravities in an hourglass mission. In Section 4, the gravitational dependency of adhesive force is analyzed and discussed. Section 5 concludes the paper by encapsulating the key findings and suggesting future research directions.

2. DEM models and calibration

2.1. Physical models

The DEM is a numerical simulation method in which a granular material is modeled as an aggregate of discrete particles. Solving for the motion of individual particles at each instant enables the analysis of the overall behavior of granular material and the interactions between particles or between particles and target objects (e.g., rover wheels). In this study, we used the commercial software Ansys Rocky[7]. For the force models governing the interactions between particles, we adopted the Hertzian spring-dashpot model and the Mindlin-Deresiewicz model for the normal and tangential directions, respectively. These models accurately simulate the dynamic responses of granular materials because they are both nonlinear spring-dash systems. In addition to these fundamental force models, we introduced a rolling resistance model to express the actual shape of the granular material and its resistance to rotation. This inclusion added a realistic factor to the simulation by accounting for the intrinsic characteristics of real-world particles.

Particles are subject to attractive forces, such as van der Waals and electrostatic forces. These can be collectively modeled in the DEM as adhesive forces F. In this study, the constant model was used, defined by the following equation:

$$F = \begin{cases} f_{\mathrm{adh}} g \min(m_1, m_2), & s \le \delta_{\mathrm{adh}} \\ 0, & s > \delta_{\mathrm{adh}} \end{cases}, \quad (1)$$

where f_{adh} represents the adhesion coefficient relative to the weight, and g is the gravitational acceleration. m_1 and m_2 are the masses of the particles in contact. s is the contact overlap and δ_{adh} shows the distance threshold at which the adhesive force acts between the particles. This modeling approach enables us to understand the impact of adhesive forces in a gravitational context, which is crucial in simulating the behavior of regoliths, especially in low-gravity environments such as the Moon or Mars.

2.2. Calibration of DEM parameters

To conduct a valid simulation using DEM, quantitative evaluations and validations must be performed by comparing them with experimental results. In this study, we calibrated the DEM parameters comprehensively in three steps: preconditioning, DEM parameter tuning, and validation.

2.2.1. Preconditioning

Based on particle density test data acquired by Ozaki et al.[6], the particle density in our simulations was treated as a fixed DEM parameter of 3.827 g/cm^3. Three representative diameters were statistically chosen from the test results for the particle size distribution. Specifically, we approximated the measured mass-frequency ratio shown in **Figure 1(a)** using a Gaussian function. We then chose the mean particle size of the Gaussian fitting and the sizes corresponding to the mean ± one standard deviation as the representative diameters. **Figure 1** shows the mass frequencies and cumulative mass ratios for the experimentally obtained and statistically selected representative particle diameters. The three representative diameters chosen in this study were 222, 258, and 294 μm, with mass ratios of 27.4%, 45.2%, and 27.4%, respectively. The particle size was scaled up by a factor of six during the tuning and validation of the DEM parameters for computational efficiency. In addition, the distance threshold δ_{adh} for the adhesive force model was fixed at 10 nm.

2.2.2. DEM parameter tuning

A direct shear test was conducted to tune the DEM parameters. The direct shear test enabled the acquisition of two characteristics: the peak strength and residual strength. The peak strength depends on the initial packing density of the granular material before the test begins[8]. However, Afzali-Nejad et al. reported that the residual strength was constant regardless of the initial packing[9]. Therefore, we tuned the DEM parameters based on the three correlation diagrams shown in **Figure 2**. **Figure 2(a)** and **(b)** correspond to the peak strength. The black squares represent the experimental results, and the gray shaded areas represent the 95% confidence intervals estimated from the experimental results. **Figure 2(c)** illustrates the residual strength,

and the gray-shaded area represents the 95% confidence ellipse calculated from the experimental results. The goal of this tuning was to ensure that the simulation results fell within the gray-shaded areas. A trial-and-error approach was employed to tune the DEM parameters. The circles in **Figure 2** represent the simulation results. For both the loose- and dense-packing states, DEM parameters that fit within the 95% confidence intervals and ellipses in all three correlation diagrams could be found.

2.2.3. Validation

A minimum density test was conducted to evaluate the calibrated parameters. The mean minimum bulk density obtained in the previous study[6] was 2.116 g/cm^3. However, the simulation results obtained using the calibrated parameters yielded 2.152 g/cm^3. Consequently, the error rate was less than 2%, indicating that valid results were obtained.

The DEM parameters obtained through the above process are summarized in **Table 1**.

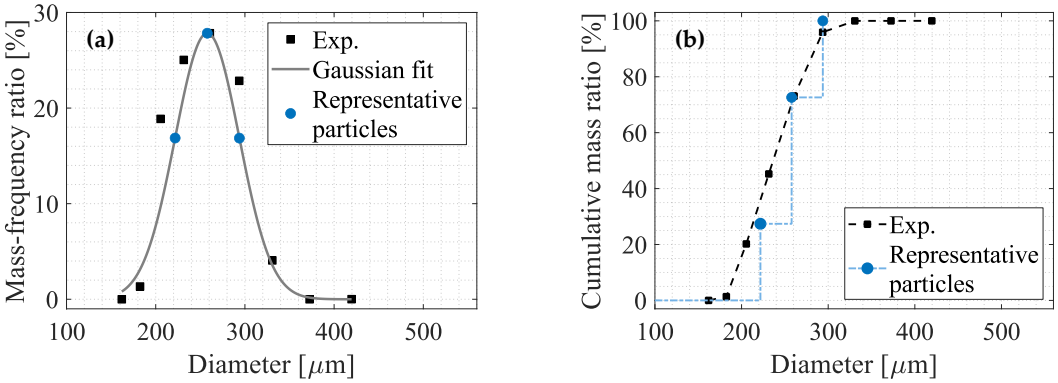

Figure 1. Representative particle diameters of alumina beads. (a) shows mass−frequency ratio, and (b) shows cumulative mass ratio.

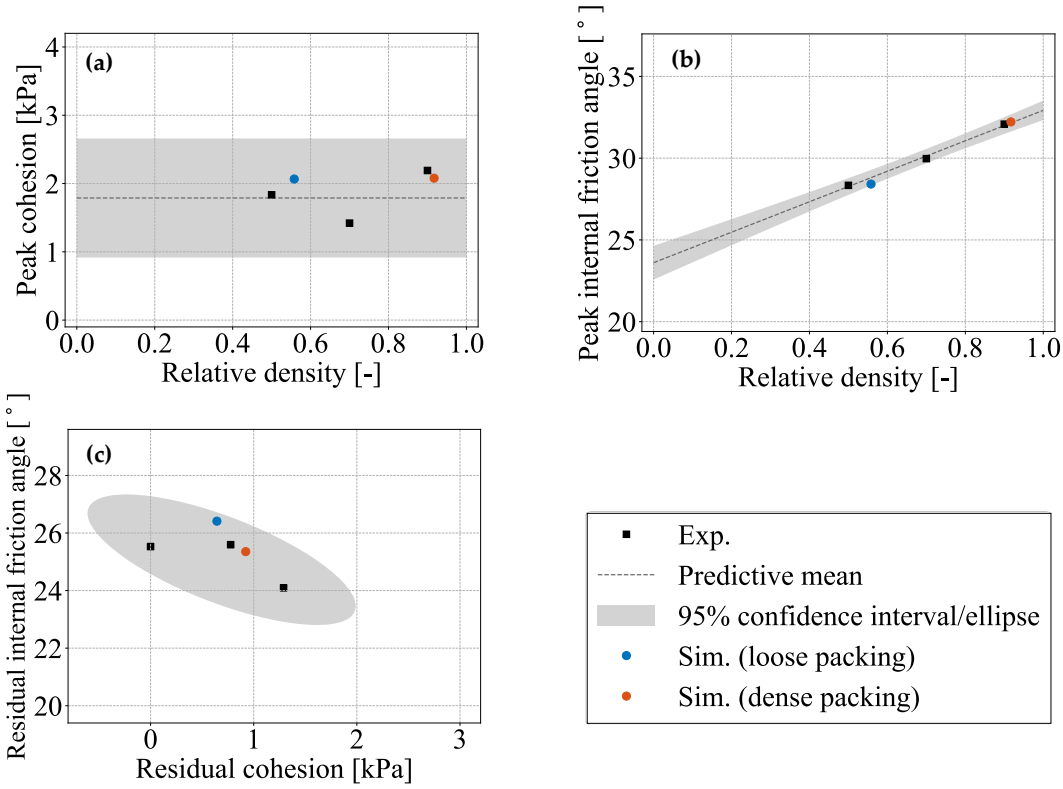

Figure 2. Experimental and simulated results in the direct shear test. (a) and (b) show the peak strength. (c) shows the residual strength.

Table 1. Calibrated discrete element method parameters for alumina beads.

Density [g/cm³]	3.827	
Diameter [μm]	222, 258, 294	
Mass ratio [%]	27.4, 45.2, 27.4	
Young's modulus [MPa]	20	
Poisson's ratio [-]	0.3	
Rolling resistance [-]	0.13	
	Particle-particle	Particle-solid boundary
Static friction coefficient [-]	0.34	0.33
Dynamic friction coefficient [-]	0.34	0.33
Restitution coefficient [-]	0.38	0.3
Adhesion coefficient [-]	0.015	0
Distance threshold [nm]	10	0

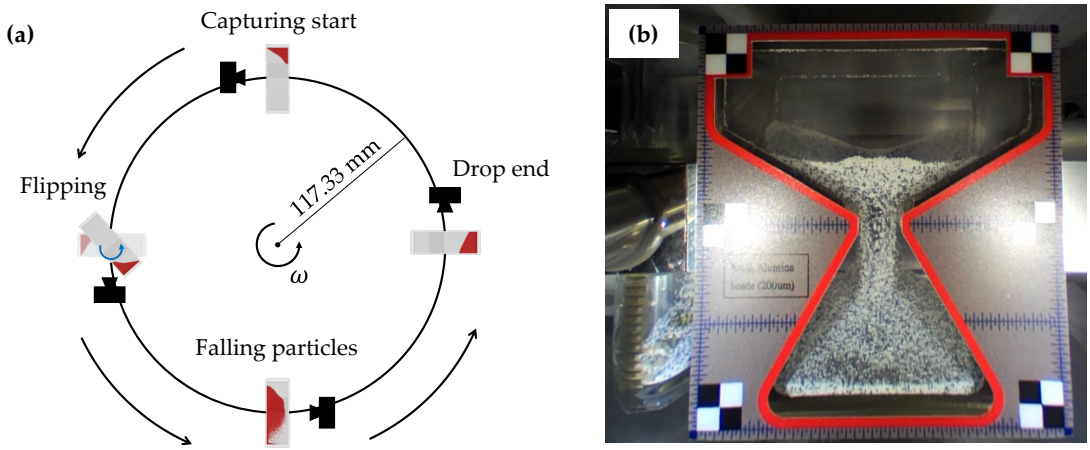

Figure 3. Hourglass experiments overview. Artificial gravity is generated by controlling the centrifuge's rotation velocity, and the particle flow is captured by a camera, as shown in (a). (b) shows a snapshot as particles fall.

3. Hourglass experiments and simulation results

3.1. Hourglass experiments overview

The hourglass mission was conducted on the ISS. During the mission, a centrifuge installed in the Japanese Experimental Module of the ISS was used to generate stable artificial gravity. This innovative setup ensures high-quality, long-term, and stable artificial gravity conditions. By controlling the centrifuge's angular velocity ω as shown in **Figure 3(a)**, the mission produced arbitrary levels of artificial gravity. In this specific campaign, gravity levels were achieved from 0.063 G to 2.0 G. Moreover, an onboard camera capable of capturing at 25 frames per second was installed on the front of the hourglass. Figure **3(b)** shows an example snapshot captured using this camera. Therefore, the alumina beads can be observed and analyzed as they fall within the hourglass, which is maintained in a vacuum under various artificial gravity conditions. This study used experimental results in six artificial gravities of 0.063 G, 0.17 G, 0.38 G, 0.50 G, 0.75 G, and 1.0 G to compare with simulation results.

3.2. Comparison of results

We consider the findings derived from the hourglass mission, focusing primarily on the angle of repose (AoR) and mass flow rate. These results are compared with the simulation results obtained using the DEM parameters calibrated in Section 2.2.

3.2.1. AoR results

The AoR was estimated from the heights of the alumina beads at the front and back of the hourglass, as shown in **Figure 4(a)**. However, in the simulation, these angles were calculated through a linear approximation of the slope as viewed from the side, as shown in **Figure 4(b)**. **Figure 5** shows the results of the AoR measured in the experiments and simulations. **Figure 5** confirms that AoR is an almost constant value regardless of gravity, which is the same as in previous research[4,5]. Moreover, even without adjusting the adhesive force, the experimental and simulation results were almost identical. Therefore, we suggest that granular materials behave similarly, regardless of gravity, with respect to static characteristics such as AoR.

3.2.2. Mass flow rate results

The mass flow rate v_m is calculated as:

$$v_m = \frac{m}{t_e - t_0}, \tag{2}$$

where m is the mass of the alumina beads packed in the hourglass (6.72 g). t_0 is the time when the hourglass is perpendicular to the direction of artificial gravity during its flip. t_e is the time when the alumina beads are depleted from the upper part of the hourglass or when they stop moving.

Figure 6 shows the mass flow rate results for different artificial gravities. The analysis revealed that the mass flow rate decreased with the decreasing gravity. This trend was also observed in the simulation results. However, a noticeable discrepancy was found between the experimental results and simulation findings in quantitative terms. This discrepancy suggests that the gravitational dependence of the adhesion force must be considered to accurately represent the dynamic behavior of granular materials.

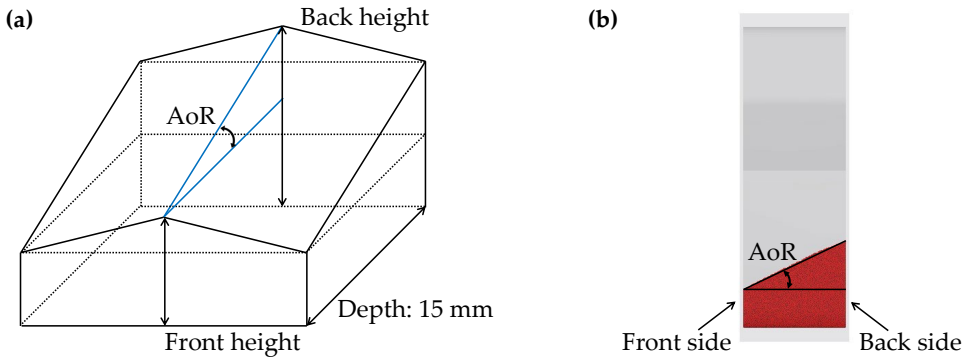

Figure 4. Angle of repose (AoR) measurement methods for (a) experiments and (b) simulations.

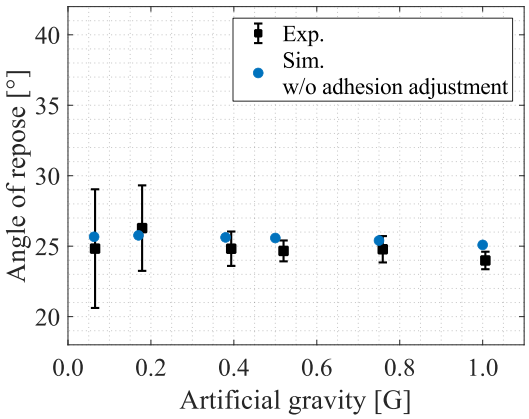

Figure 5. Results of the angle of repose.

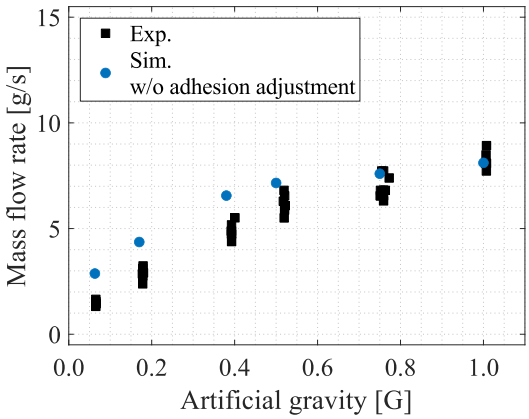

Figure 6. Results of mass flow rate.

4. Adhesive force dependency on gravity

The previous section discussed the discrepancy between the experimental and simulation results for the mass flow rate. Therefore, we aligned the two by adjusting the adhesion coefficient f_{adh}. **Figure 7** confirms that a reduction in the adhesive force was desirable as gravity decreased. Moreover, a greater adhesive force must be provided when considering dynamic characteristics, such as the mass flow rate, compared with when considering static characteristics, such as the AoR. From the above results, the adhesive force has conceivable gravity and velocity dependencies. Generally, from the law of conservation of mechanical energy, the velocity of an object falling freely at a certain distance is proportional to $\sqrt{g}$. Therefore, the mass flow rate v_{m} is also considered proportional to $\sqrt{g}$, as shown in **Figure 6**. However, individual differences in velocity are likely to occur as the particle velocity increases. This leads to more opportunities for the particles to come into contact, resulting in a relative increase in the contact area. As a result, van der Waals forces increase. The likelihood of deformation during particle collisions owing to the faster velocity might also contribute to the increase in van der Waals forces. Furthermore, the increased probability of individual velocity differences may result in a greater electrostatic force. These considerations conclude that a higher particle velocity increases the adhesive force. In contrast, in a state with static characteristics, such as the AoR, where the relative velocity of the particles is zero, the adhesive force is neglected, and gravity dependency is barely observed (see **Figure 7**).

Therefore, we focus on the gravity and velocity dependencies of the adhesive force. According to Ozaki et al.[6], the relationship between the mass flow rate v_{m} and gravity magnitude $G = g/g_{\mathrm{E}}$, where g_{E} is the gravitational acceleration on Earth, can be expressed as

$$v_{\mathrm{m}} = \alpha G^{\beta+0.5}, \tag{3}$$

where α and β are coefficients that depend on granular material. These coefficients were obtained from the experimental results. In the case of alumina beads, α and β were 15.41 g/s and 0.0836, respectively. The dotted line in **Figure 7** represents the linear fitting results for the adhesive force adjusted in the simulations. The high value of the coefficient of determination R^2 (0.980) suggests a relationship between the adhesion force and the degree of gravity, as follows:

$$F = aG + b, \tag{4}$$

where a and b are the coefficients that depend on the granular material. a and b are 7.31 μN and 0.09 μN, respectively. b can be neglected as it is infinitesimally small. From **Equation 3** and **4**, the relationship among the adhesive force F, mass flow rate v_{m}, and gravity magnitude G can be expressed as

$$F = a\left(\frac{v_{\mathrm{m}}}{\alpha}\right)^2 G^{-2\beta}. \tag{5}$$

Thus, adhesive force should not be considered when dealing with static characteristics when no velocity is present, according to the above equation. However, when dealing with the dynamic characteristics, the influence of gravity must be considered. Furthermore, if v_{m} is constant, a reduction in gravity increases the adhesive force, suggesting that the dominance of the adhesive force increases when gravity is low.

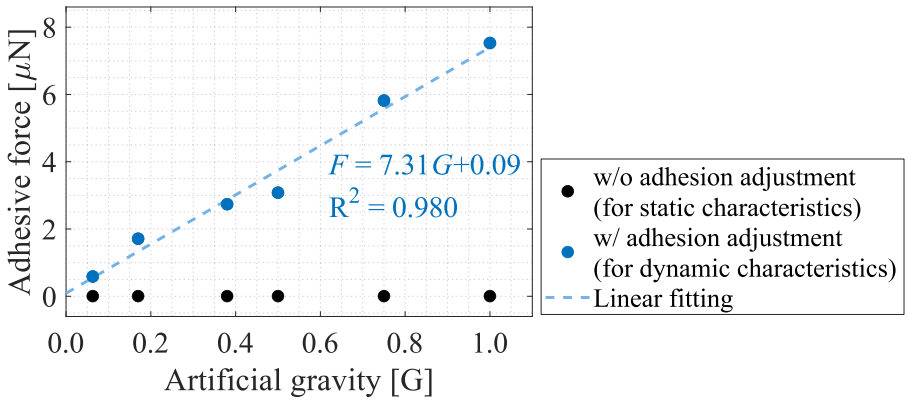

Figure 7. Gravitational dependency of adhesive force F. G is the magnitude of gravity and R^2 indicates the coefficient of determination.

5. Conclusion

Based on the Hourglass mission conducted on the ISS, we analyzed the magnitude of the adhesive force acting between alumina beads using DEM. The results revealed that, when dealing with static characteristics, the adhesive force is small and remains constant, regardless of gravity. In contrast, gravity and velocity dependencies were observed in the dynamic characteristics of the particles. When gravity is low, the particle velocity is low, and although the adhesive force is small, the dominance of gravity over the velocity becomes significant. From these results, we conclude that a distinct difference in the adhesive force should be provided whether dealing with the static or dynamic characteristics of granular materials. Specifically, in analysis of static characteristics, such as in the selection of a landing site for spacecraft, there is no need to consider the gravity dependency of the adhesive force. Conversely, in the analysis of dynamic characteristics, such as in the analysis of regolith dispersion during the takeoff and landing of spacecraft, the gravity dependency of the adhesive force must be considered, and the quantitative results obtained in this study can be applied. However, the boundary conditions of the particulate matter velocity that determine whether the adhesive force must be considered remain unclear. In scenarios that require handling both the static and dynamic characteristics of particulate matter, such as the driving analysis of planetary exploration or human-pressurized rovers, careful consideration of the magnitude of the interparticle adhesive force is necessary. Moving forward, further analyses will be conducted to determine the boundary velocity at which the magnitude of the adhesive force should be considered. Additionally, we aim to verify the validity of a model that considers the gravity and velocity dependency of the adhesive force, and to construct an adhesive force model that encompasses both the static and dynamic characteristics of granular materials.

Acknowledgment

We express our special thanks to Prof. Ozaki of Yokohama National University and Prof. Kobayashi of Ritsumeikan University for providing detailed soil test data. This study was supported by JSPS KAKENHI (grant number: JP23KJ1901).

References

1) R.A. Kerr: Mars Rover Trapped in Sand, But What Can End a Mission? Science, **324** (2009) 998, DOI: 10.1126/science.324_998.
2) C. Immer, P. Metzger, P.E. Hintze, A. Nick and R. Horan: Apollo 12 Lunar Module exhaust plume impingement on Lunar Surveyor III. Icarus, **211** (2011) 1089, DOI: 10.1016/j.icarus.2010.11.013.
3) D.E. Brownlee, W. Bucher and P. Hodge: Part A, Primary and Secondary Micrometeoroid Impact Rate on the Lunar Surface: A Direct Measurement. In Analysis of Surveyor 3 material and photographs returned by Apollo 12, National Aeronautics and Space Administration (1972).
4) H. Nakashima, Y. Shioji, T. Kobayashi, S. Aoki, H. Shimizu, J. Miyasaka and K. Ohdoi: Determining the angle of repose of sand under low-gravity conditions using discrete element method. J. Terramech, **48** (2011) 17, DOI: 10.1016/j.jterra.2010.09.002.
5) J.P. Marshall, R.C. Hurley, D. Arthur, I. Vlahinic, C. Senatore, K. Iagnemma, B. Trease and J.E. Andrade: Failures in sand in reduced gravity environments. J. Mech. Phys. Solids, **113** (2018) 1, DOI: 10.1016/j.jmps.2018.01.005.
6) S. Ozaki, G. Ishigami, M. Otsuki, H. Miyamoto, K. Wada, Y. Watanabe, T. Nishino, H. Kojima, K. Soda, Y. Nakano, M. Sutoh, T. Maeda and T. Kobayashi: Granular flow experiment using artificial gravity generator at International Space Station. npj Microgravity, **9** (2023) 61, DOI: 10.1038/s41526-023-00308-w.
7) Ansys Inc.: DEM Technical Manual, Ansys Rocky 2023 R2 (2023).
8) J. Katagiri, T. Matsushima and Y. Yamada: Variations in shear behavior among specimens with different packing patterns. Granular Matter, 16 (2014) 891, DOI: 10.1007/s10035-014-0530-4.
9) A. Afzali-Nejad, A. Lashkari and P.T. Shourijeh: Influence of particle shape on the shear strength and dilation of sand-woven geotextile interfaces. Geotext. Geomembr., **45** (2017) 54, DOI: 10.1016/j.geotexmem.2016.07.005.